

# Journal of Materials Chemistry A

Accepted Manuscript



This is an *Accepted Manuscript*, which has been through the Royal Society of Chemistry peer review process and has been accepted for publication.

*Accepted Manuscripts* are published online shortly after acceptance, before technical editing, formatting and proof reading. Using this free service, authors can make their results available to the community, in citable form, before we publish the edited article. We will replace this *Accepted Manuscript* with the edited and formatted *Advance Article* as soon as it is available.

You can find more information about *Accepted Manuscripts* in the [Information for Authors](#).

Please note that technical editing may introduce minor changes to the text and/or graphics, which may alter content. The journal's standard [Terms & Conditions](#) and the [Ethical guidelines](#) still apply. In no event shall the Royal Society of Chemistry be held responsible for any errors or omissions in this *Accepted Manuscript* or any consequences arising from the use of any information it contains.

# An epidermal alkaline rechargeable Ag-Zn printable tattoo battery for wearable electronics

Sheela Berchmans<sup>a,b</sup>, Amay J. Bandodkar<sup>a</sup>, Wenzhao Jia<sup>a</sup>, Julian Ramirez<sup>a</sup>, Ying S. Meng<sup>a\*</sup>, Joseph Wang<sup>a\*</sup>

<sup>a</sup> Department of Nanoengineering, University of California San Diego, 9500 Gilman Drive, La Jolla, CA 92093 (USA)

<sup>b</sup> EEC Division (Biosensors group), CSIR-Central Electrochemical Research Institute, Karaikudi, 63006, Tamilnadu, India

\*The authors to whom correspondence should be addressed E-mail: josephwang@ucsd.edu, shirleymeng@ucsd.edu

## Abstract

Herein we report for the first time the fabrication of a rechargeable, benign, skin-worn Ag-Zn tattoo battery using unconventional materials, such as screen printed electrodes, temporary tattoo paper, alkaline gel electrolytes and a PDMS cover for sealing the battery. The tattoo battery can be easily worn by a person for powering wearable devices. Detailed characterization of a typical Ag-Zn tattoo cell reveals a capacity density in the range 1.3- 2.1 mAhcm<sup>-2</sup> and stability up to 13 cycles. The tattoo cell exhibits a stable open circuit voltage of 1.5 V over a 5 days period and endures repeated stretching and bending strain cycles with minimal decrement in its performance. The lateral arrangement of the negative and positive electrodes allows the integration of several cells into a battery in series or parallel arrangements for tuning the discharge capacity and voltage to the desired values. The practical nature of the tattoo battery was illustrated by applying it to a human subject's skin followed by lighting a red LED. The epidermal tattoo battery thus meets the demands of wearable power sources, including mechanical compliance and tunable discharge capacity, to power body-worn electronic devices.

**Keywords:** Printed electronics, thin-film alkaline batteries, wearable devices, temporary tattoo technology.

## Introduction

The development of wearable health systems has made considerable progress in recent years. The advent of wearable electronics and wireless networks have facilitated the real-time on-body monitoring of vital physical signs<sup>1</sup>, such as blood pressure, heart rate, or skin temperature, as well as of chemical parameters like lactate<sup>2</sup>, pH<sup>3</sup> and sodium<sup>4</sup>. However, powering such on-body sensors is a challenging problem which can be addressed by self-powered devices or by wearable

1 power sources. Recent efforts have led to innovative solutions such as flexible thin-film  
2 batteries<sup>5,6</sup>, piezoelectric nanogenerators<sup>7</sup>, wearable solar cells<sup>8,9</sup>, microsupercapacitors<sup>10</sup>,  
3 wearable thermoelectric generator<sup>11</sup>, epidermal biofuel cells<sup>12</sup> and endocochlear-potential-based  
4 biobatteries.<sup>13</sup> Of these, thin-film wearable batteries hold the highest promise as they can provide  
5 high power levels at low cost and can be recharged for repeated use. Despite of their tremendous  
6 potential, much needs to be achieved in the wearable battery field to keep pace with the rapidly  
7 growing field of wearable and implantable devices. Merger of materials science and energy  
8 technology can ultimately lead to the development of ultrathin, safe energy storage devices that  
9 can be easily incorporated on to clothes, eye glasses, wrist watches, and even skin to power  
10 modern wearable gadgets.<sup>14</sup>

11  
12 Lack of compliant rechargeable wearable batteries that conform well to the contours of the body  
13 is a major bottleneck in the development of wearable electronics. Conventional batteries consist  
14 of rigid metallic substrates and thus cannot be directly used as wearable skin-worn power  
15 sources. The main components of the battery, viz., electrode, separator and electrolyte, thus need  
16 to be modified for enduring complex body movements without compromising the battery's  
17 performance. Construction of energy devices based on unconventional substrates, such as  
18 polymer films, metal foils, paper, textile or rubber slabs, is becoming popular as indicated from  
19 the current literature. Particular attention has been given to the development of flexible Li ion  
20 batteries due to their high open circuit voltage, high energy density, low self-discharge and lack  
21 of memory effect. Different versions of the flexible Li battery, such as stretchable battery with  
22 serpentine interconnects withstanding 300% stretchability<sup>15</sup>, wearable textile-based Li battery<sup>16</sup>,  
23 paper-based origami Li battery<sup>17</sup>, CNT and CNT composite based Li batteries on paper supports  
24 <sup>18,19</sup> and cable type Li batteries,<sup>20</sup> have been reported in the literature. Dry batteries (Zn-carbon,  
25 Leclanche batteries), on the other hand, are considered as economic and environmental friendly.  
26 Compliant versions of dry batteries have been reported with electro spun carbon mats as cathode,  
27 along with Zn foil anode in the presence of polyethylene oxide (PEO) electrolyte containing  
28 TiO<sub>2</sub> nanoparticles<sup>21</sup> and also with stretchable carbon-paste based current collectors where a Zn  
29 paste (made of Zn, carbon black and xanthan gel) served as anode and MnO<sub>2</sub> paste (made of  
30 MnO<sub>2</sub>, carbon black and electrolyte paste) acting as cathode<sup>22</sup>. Alkaline batteries are similar to  
31 dry batteries and flexible versions of such systems have been fabricated using conductive textile  
32 substrates for wearable applications.<sup>5,23-25</sup> Ag-Zn batteries are being used in small and large scale  
33 applications. A stretchable Ag-Zn battery based on embedded nanowire elastic conductors was  
34 recently reported.<sup>26</sup> However; they can provide a maximum areal capacity of only 0.11 mAhcm<sup>-2</sup>  
35 due to the low areal density of nanowire configuration. Other type of battery systems, such as  
36 Zn-air<sup>27</sup>, Al-Cu<sup>28,29</sup> and Mg-Cu<sup>30,31</sup> based on paper supports, have also been reported. Some of  
37 the paper-based battery systems have been integrated into microfluidic channels and  
38 microelectrochemical sensing platforms for the development of self-powered analytical  
39 systems<sup>32-36</sup>.

40

1 The present article reports on the fabrication and characterization of an epidermal tattoo-based  
2 Ag-Zn rechargeable battery for powering wearable electronics. Ag-Zn batteries belong to a class  
3 of mature battery systems that provide high power and are preferred for critical large scale  
4 applications in space, underwater and military as well as on smaller scale, for example, powering  
5 watches. Ag-Zn cells are safer as they make use of the water-based electrolytes, unlike Li-ion  
6 batteries which rely on hazardous nonaqueous solvents. Zinc-based batteries also provide an  
7 attractive alternative to Li-ion batteries because of the extensive global reserves of Zn. Hence,  
8 Ag-Zn cells represent an attractive choice for use in wearable, flexible devices. Though, silver is  
9 relatively expensive, the virtues of an Ag-Zn galvanic cell, namely, lower toxicity, ability to  
10 work without glove-box and possibility to develop all-printed batteries make it a better choice for  
11 wearable applications as compared to its Li counterparts. The new skin-worn Ag-Zn tattoo cell,  
12 inspired by our earlier work on tattoo-based electrochemical sensors<sup>3,4</sup>, has been realized by  
13 amalgamating diverse screen printing, temporary tattoo and thin-film battery technologies  
14 (Figure 1). The tattoo battery is referred to as an “*epidermal*” device since it adheres directly to  
15 the epidermis (outermost layer of the human skin) similar to a commercial temporary tattoo. As  
16 these devices can be applied directly to the skin, they offer great levels of freedom to the wearer  
17 for applying them at any location on the skin. Such freedom is not feasible in case of plastic and  
18 textile-based battery devices. Additionally, the tattoo batteries are fabricated using inexpensive  
19 screen printing technology and which lowers the device cost significantly. The versatility of the  
20 printing technology offers great freedom to develop tattoo-based batteries of any shape and  
21 allows several cells to be connected in parallel and/or series combination to alter the total voltage  
22 and current. Tattoo papers are also relatively cheap, thin, light weight, flexible, biocompatible  
23 and biodegradable.

## 24 Experimental

25

### 26 Materials

27

28 The following chemicals were used as received without further purification: ZnSO<sub>4</sub> (Fluka),  
29 H<sub>3</sub>BO<sub>3</sub> (EMD), Sulphuric acid (EMD), Ag plating solution (Technic Inc. Rhode Island), KOH  
30 (Sigma-Aldrich), LiOH (Sigma-Aldrich), Poly acrylic acid (Sigma-Aldrich), Poly acrylic acid-  
31 partial potassium salt (Sigma-Aldrich), ZnO (Sigma-Aldrich).

32

33

### 34 Fabrication of Ag-Zn cell

35

36 A typical Ag-Zn tattoo cell was constructed using ink jet tattoo paper (Papilio, HPS LLC,  
37 Rhome, TX) as support. Electrode patterns were designed in AutoCAD (Autodesk, San Rafael,  
38 CA) and outsourced for fabrication on stainless steel through-hole 12 in.×12 in. framed stencils  
39 (Metal Etch Services, San Marcos, CA). A sequence of the transparent insulator (DuPont 5036  
40 Wilmington, DE), Ag layer (Dupont 5874, Wilmington, DE) as reference electrode, carbon layer

1 (E3449, Ercon, Inc., Wareham, MA) as current collector followed by a final layer of transparent  
2 insulator for defining electrode active area was screen printed employing an MPM-SPM  
3 semiautomatic screen printer (Speedline Technologies, Franklin, MA). Three electrode  
4 configuration facilitates electrodeposition of the active materials Zn (negative electrode) and Ag  
5 (positive electrode) separated by 1cm. A pair of three electrodes was printed laterally on a tattoo  
6 paper which provides scope for integrating arrays of cells into a battery. The electrochemical  
7 experiments were performed using microAutolab type III (Metrohm, the Netherlands). Ag and  
8 Zn were electrodeposited on the active carbon area ( $\phi=3\text{mm}$ ) at a current density of  $-1.75\text{ mA}$  for  
9 600secs using plating solutions of Ag and Zn respectively. The composition of the Zn plating  
10 solution is as follows:  $80\text{ g l}^{-1}\text{ ZnSO}_4$ , and  $20\text{ g l}^{-1}\text{ H}_3\text{BO}_3$  solutions (buffered to  $\text{pH} = 2.5$  with  
11 sulfuric acid. The Ag plating solution was obtained from Technic Inc. , Rhode island. After  
12 electrodeposition the counter and reference electrodes were masked by a thin film of epoxy and  
13 two wells of epoxy were created around the Ag and Zn electrodes which were then filled with  
14 poly acrylic acid gel electrolytes. The Ag electrode was covered with gel containing 3% poly  
15 acrylic acid (PAA) containing  $6\text{MKOH} + 1\text{M LiOH}$ . The Zn electrode was covered with a gel  
16 containing 10% poly acrylic acid partial potassium salt (PAA-K) containing  $6\text{M KOH} + 1\text{M}$   
17  $\text{LiOH}$  saturated with  $\text{ZnO}$ . The gap between the electrode wells was covered with the gel  
18 containing 3% poly acrylic acid (PAA) containing  $6\text{MKOH} + 1\text{M LiOH}$  which provides the  
19 required ionic contact between the anode and cathode compartments. The electrodes surrounded  
20 by the gel was subsequently covered with a PDMS film and sealed with epoxy glue. The casting  
21 solution was prepared by mixing PDMS prepolymer and the initiator from the Sylgard184  
22 silicone elastomer kit in the 10:1 ratio followed by curing at 90 degrees for 10 mins. The film of  
23 the required thickness was obtained by casting the solution on a glass plate. The final thickness  
24 of the device was approximately 2mm. The tattoo battery was transferred to receiving substrates  
25 (Gore-tex<sup>®</sup> fabric or human skin) in a manner discussed in our earlier work<sup>2,3</sup>. Prior to the on-  
26 body test, consent was obtained from the human subject. The test was performed in compliance  
27 with the protocol that was approved by the institutional review board (IRB) at the University of  
28 California, San Diego. It should be pointed out that the release agent-coated tattoo base paper is  
29 used as a support to fabricate the entire tattoo battery. The tattoo battery transfer process  
30 involved applying a thin layer of transparent adhesive to the device, followed by its adherence to  
31 the receiving substrate. Finally, the tattoo paper was gently removed by dabbing the paper with  
32 water.

33

### 34 **Electrochemical measurements**

35

36 Charge –discharge studies of the Ag-Zn tattoo cell were carried out galvanostatically  
37 (microAutolab type III, Metrohm, the Netherlands) by applying a current of  $100\mu\text{A}$  or  $150\mu\text{A}$ .  
38 The charge –discharge cycles were carried out in the voltage range 2.05 V to 0.8V. Between  
39 each cycle an interval of 10 minutes was given during which open circuit voltage (OCV) of the  
40 cell was monitored. Electrochemical impedance measurements were carried out using CH

1 instrument electrochemical analyser (CHI 660D CH Instruments, Austin, TX)) in the frequency  
2 region 0.1 Hz to 1 MHz at an AC amplitude of 10 mV. The measurements were recorded at the  
3 open circuit voltage of the cell.

4

### 5 **Mechanical testing**

6

7 The mechanical resiliency of the tattoo cell was examined by subjecting the cell to repeated  
8 bending and stretching after transferring the cell to a stretchable Gore-tex<sup>®</sup> fabric. In the case of  
9 stretching study, the tattoo cell was stretched along the length of the electrodes at a controlled  
10 speed of 0.1mm/s and an increasing strain from 0 to 11.1% was applied to the tattoo cell using a  
11 tensile test machine (Instron<sup>®</sup> 5900 Series Model 5982, Norwood, MA). The effect of  
12 mechanical deformations was monitored by discharge using linear polarisation measurements  
13 between the voltage limits 2.05 V and 0.8 V at a scan rate of 2mV/s and by galvanostatic  
14 discharge method. The discharge test using linear polarisation was performed after every 5  
15 fatigue cycles for a total of 25 cycles. The bending study comprised of subjecting the tattoo cell  
16 to a bending stress of 180<sup>0</sup> along the latitude. The tattoo cell was repeatedly bent perpendicular  
17 to the length of the electrodes for a total of 100 fatigue cycles and the discharge data using linear  
18 polarisation was recorded after every 20 bending iterations. A galvanostatic discharge was  
19 carried out at the completion of all the fatigue cycles during stretching and bending.

20

### 21 **SEM**

22

23 Scanning electron microscopy (SEM) images were taken using a Phillips XL30 ESEM  
24 instrument with an acceleration potential of 20 kV. All SEM samples were sputtered with  
25 iridium for 7s before imaging. SEM images were recorded for the electrodeposited positive and  
26 negative electrodes (Ag and Zn electrodes on carbon collectors) and also for the positive and the  
27 negative electrodes removed from the cell after complete discharge.

28

29

## 30 **Results and Discussion**

31

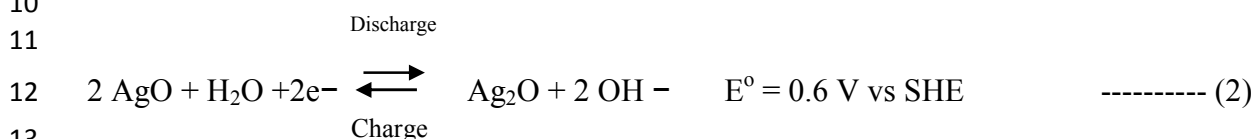
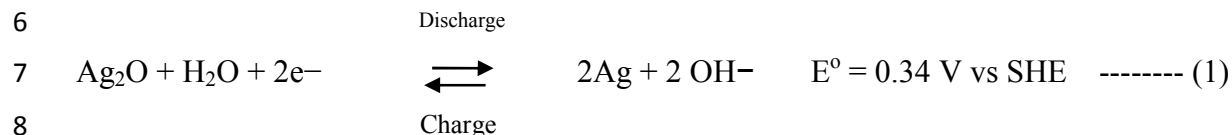
### 32 **Redox reactions at the negative and positive electrode**

33

34 Figure 2A shows the typical redox reactions of the Ag-Zn tattoo cell and the cyclic  
35 voltammograms corresponding to the negative (Zn) and the positive (Ag) electrodes. The cyclic  
36 voltammograms shown in Figure 2B and C represent the electrochemical response of the  
37 negative and positive electrodes in 6M KOH + 1M LiOH electrolyte at a scan rate of 5 mV/s.  
38 The response of the negative electrode shows the redox behaviour of the Zn electrode  
39 constituting of the Zn/Zn(OH)<sub>2</sub> redox couple. The redox reaction is quasi reversible as seen from  
40 the voltammogram. The response of the positive electrode corresponds to the formation of the



1 two oxides, Ag<sub>2</sub>O and AgO (Figure 2C). The redox couples that exist at the positive electrode are  
 2 AgO/Ag<sub>2</sub>O and Ag<sub>2</sub>O/Ag. Thus, the reduction of AgO to Ag occurs in two stages. The Ag<sub>2</sub>O/Ag  
 3 redox couple is reversible and the redox couple AgO/Ag is quasi reversible as seen from the  
 4 voltammogram:



### 15 Discharge Characteristics of the Ag-Zn tattoo cell

17 The discharge characteristics of a typical Ag- Zn tattoo cell are shown in Figure 3 (A-C). The  
 18 Ag-Zn tattoo cell was subjected to galvanostatic charge–discharge cycling in the voltage limits  
 19 between 2.05 and 0.8 V at the rate of 1.4 mAcm<sup>-2</sup>. The variation of cell voltage during a charge-  
 20 discharge cycle is illustrated in Figure 3A. The two plateau regions at 1.7 and 2.0 V observed  
 21 during charging correspond to the two stages of oxidation of the positive electrode (Reactions (1)  
 22 and (2), respectively). The sharp rise observed during charging corresponds to the formation of  
 23 high resistance Ag<sub>2</sub>O layer and the formation of the second plateau corresponds to the formation  
 24 of AgO<sup>37</sup>. The voltage spike observed between the first and the second plateau is due to highly  
 25 resistive Ag<sub>2</sub>O completely surrounding the electrode. Upon complete charging the sudden sharp  
 26 voltage rise is attributed to the electrolysis of water. During discharge, there is a gradual decrease  
 27 of the voltage from 1.8 to 1.5 V. The voltage remains fairly constant at 1.5V for major section of  
 28 discharging followed by a rapid decrease at the end. The gradual decrease of voltage from 1.8 to  
 29 1.5 V is due to the first-stage reduction of AgO to Ag<sub>2</sub>O (Reaction (2)), wherein these two  
 30 compounds form a solid solution. The decrease in voltage is due to an increase in concentration  
 31 of Ag<sub>2</sub>O in the AgO–Ag<sub>2</sub>O solid solution. The second discharge-plateau at 1.5 V is due to the  
 32 constant concentration of Ag(OH)<sub>2</sub>. The potential of the negative electrode, namely Zn/Zn(OH)<sub>2</sub>  
 33 is expected to be constant throughout the discharge due to the constant concentration of  
 34 supersaturated Zn(OH)<sub>4</sub><sup>2-</sup> ions.

35 The discharge capacity over 13 cycles is shown in Figure 3B. An average discharge capacity of  
 36 1.48 mA hcm<sup>-2</sup> is observed over 8 cycles. Thereafter, the capacity starts decreasing and reaches a  
 37 value of 0.5 mA hcm<sup>-2</sup> at the 13<sup>th</sup> cycle. The charge –discharge efficiency is shown in Figure 3C.  
 38 The efficiency increases from 69% for the first cycle and remains close to 90% up to 12 cycles  
 39 and finally goes down to 72%. A maximum volumetric capacity of 2.94 mA hcm<sup>-3</sup> was achieved.  
 40 However, the cycling ability of the cell decreases when the cell is discharged at higher rates (for

1 example:  $2.14 \text{ mAhcm}^{-2}$ ) (See supporting information, Figure S1). The charge–discharge  
2 efficiency of the cell can be improved by suppressing hydrogen evolution at the anode, improving  
3 the electrochemical reversibility and stability of silver oxides and further optimizing the battery  
4 fabrication and sealing process. It can be shown that the power output of the tattoo cell can be  
5 improved by printing three current collectors to build a cell with an Ag-Zn-Ag configuration.  
6 The discharge capacity of such a cell was found to be  $2.1 \text{ mAhcm}^{-2}$  (See supporting information,  
7 Figure S2). This indicates that arrays of the cell can be designed by lateral printing of current  
8 collectors on a tattoo paper and integrate them into a battery depending upon the specific power  
9 requirements. The open circuit voltage (OCV) of the Ag-Zn tattoo cells were stable at 1.5 V and  
10 the life of the cell was around 3-5 days (Supporting information, Figure S3).

11

## 12 **Effect of Mechanical Deformations**

13

14 A wearable device must conform perfectly to the human body and show minimal effect on its  
15 performance due to the mechanical deformations experienced by the skin during ambulatory  
16 activities of the body. A temporary tattoo based device adheres well to the complex morphology  
17 of the human epidermis and can survive for long durations.<sup>38</sup> The mechanical resiliency of the  
18 tattoo battery was examined by subjecting it to repeated bending and stretching iterations that  
19 mimics the mechanical stress usually endured by the human epidermis.

20

### 21 ***Stretching effect***

22 The effect of stretching stress on tattoo battery performance was evaluated by applying the  
23 tattoo battery to Gore-tex<sup>®</sup> and subjecting it to increasing levels of tensile strain. The discharge  
24 characteristics of the tattoo cell was measured after every 5 stretching fatigue cycles by linearly  
25 varying the voltage from 2.05 V to 0.8 V at  $2\text{mVs}^{-1}$  (Figure 4A). The peak current corresponding  
26 to the reduction of  $\text{Ag}_2\text{O}$  to Ag decreases from  $27 \text{ mAcm}^{-2}$  to  $6 \text{ mAcm}^{-2}$  upon increasing the  
27 strain to 11.1%. At the end of stretching experiments a galvanostatic discharge is finally  
28 conducted to check the performance of the cell. After the stretching experiments the  
29 galvanostatic discharge capacity decreased to 18% of the initial discharge capacity (Figure 4 B &  
30 C).

31

### 32 ***Bending effect***

33

34 The human epidermis regularly undergoes stress generated due to bending of muscles. The  
35 effect of such bending stress was analysed on the tattoo battery by bending it by  $180^\circ$  along the  
36 latitude for up to 100 times. Similar to the stretching study, the discharge characteristics of the  
37 tattoo battery was measured after every 20 bending cycles by linearly varying the voltage from  
38 2.05 V to 0.8 V at a scan rate of  $2\text{mV/s}$ . As seen from the figure, the changes in the peak current  
39 due to reduction of  $\text{Ag}_2\text{O}$  to Ag can be ascribed to the effect of bending. After 100 bendings the  
40 current density of the  $\text{Ag}_2\text{O}/\text{Ag}$  peak decreased from an initial value of  $20 \text{ mAcm}^{-2}$  to  $14.5$   
41  $\text{mAcm}^{-2}$  (Figure 5A) and the galvanostatic discharge capacity decreased to 66% (Figure 5B and



1 C). The study thus reveals the resiliency of the tattoo cell to withstand large number of bending  
2 fatigue cycles with minimal effect on its performance. The effect of bending stress was also  
3 monitored by coupling 2 Ag-Zn tattoo cells in series to light up a red LED (operating voltage  
4 1.8V; current consumption 20 mA). Figures 5 D-G clearly demonstrate that the tattoo battery can  
5 perform very well even under extreme deformation conditions, underscoring the practical nature  
6 of the wearable tattoo battery system. (This study was performed after removal of the tattoo base  
7 paper.) It was observed that the tattoo device adhered firmly to the underlying Gore-tex<sup>®</sup>  
8 substrate even after it was subjected to repeated bending and stretching stressors. This  
9 observation emphasizes that the tattoo battery can withstand the deformations expected during  
10 real-life use of such devices.

### 11 12 **Morphology of the electrodes**

13  
14 SEM images of the active materials are presented in Figure 6. For example, Figure 6A and B  
15 displays SEM images of the electrodeposited Ag and Zn active materials, respectively, on the  
16 carbon current collector. The electrodeposited Ag electrode has a clustered nano-dendritic  
17 structure while the SEM image of Zn electrode reveals a nano-porous morphology. SEM analysis  
18 was also performed after complete discharge of the Ag-Zn cell. The effect of complete discharge  
19 on both the electrodes can be easily observed via the SEM images (Figure 6 C and D). After  
20 complete discharge the morphology of the Ag electrode transforms to nanowires and flakes from  
21 the nano-dendritic structure (Figure 6 C). This may be due to the presence of a mixture of several  
22 active components (Ag, Ag<sub>2</sub>O and AgO) on the positive electrode. On the other hand, the  
23 electrodeposited Zn on the negative electrode dissolves during the discharge process, leading to  
24 the loss of the nano-porous structure (Figure 6 D).

### 25 26 **On Body transfer of the Tattoo battery**

27  
28 This section demonstrates the epidermal application of the new tattoo battery in real-life  
29 scenarios. In this study, two tattoo cells were connected in series to power a LED. A consenting  
30 human subjected to apply the tattoo battery to his right deltoid. The tattoo transfer process is  
31 similar to our earlier reported works.<sup>2,3</sup> The tattoo battery was easily worn by the subject without  
32 any assistance. Upon transfer of the tattoo battery, a red LED (operating voltage 1.8V; Current  
33 consumption 20 mA) was turned 'ON' by connecting it in series with the skin-worn tattoo  
34 battery. Figure 7 A and B illustrate the tattoo battery in action, lighting a LED before transfer  
35 onto the skin. Figures 7 C and D show photograph of the tattoo battery transferred on to the  
36 human subject in "ON" and "OFF" states. The study demonstrates the pragmatic nature of the  
37 developed tattoo-based alkaline batteries to power devices. The epidermal tattoo batteries can be  
38 removed from the skin and applied back by using a fresh transparent adhesive for repeated use.

### 39 40 **Performance analysis**

1 Literature reveals that there is quite a lot of interesting investigations going on with the  
2 development of flexible Li-ion batteries<sup>15-20</sup>. Li-ion batteries face major challenging issues due to  
3 the flammability of the organic electrolyte, and the reactivity of the electrode materials with the  
4 organic electrolytes in case of improper use such as overcharging or short-circuiting. Alkaline  
5 Ag-Zn batteries with discharge current density of  $1.8 \text{ mAcm}^{-2}$  have been reported.<sup>39</sup> However,  
6 the rigid gold sputtered glass substrate utilized for the fabrication of these batteries limit their use  
7 for wearable applications. Recent work on stretchable Ag-Zn batteries addresses the issue body  
8 compliance.<sup>26</sup> However, the battery reveals a low discharge capacity of  $0.11 \text{ mAhcm}^{-2}$ . Though  
9 the paper reports 1000 charging cycles, the study was performed for the silver electrode and not  
10 for the entire battery system. Similarly, a fabric-based Ni-Zn battery using microfiber substrate  
11 and separator with an areal capacity of  $1.4 \text{ } \mu\text{Ahcm}^{-2}$  after four discharge cycles, has also been  
12 reported.<sup>40</sup> The present work describes a novel method to power skin electronics by building Ag-  
13 Zn batteries on temporary transfer tattoo supports. The resulting flexible tattoo-based Ag-Zn  
14 battery has a discharge capacity of  $2.1 \text{ mAhcm}^{-2}$  for 13 cycles and can endure repeated  
15 mechanical stress. Thus, the tattoo battery meets the demands of wearable electronics, offering  
16 attractive flexibility and good discharge capacity. Ag-Zn cells are less toxic and the alkaline  
17 electrolyte used in this work has been used in prior work for developing medical devices.<sup>41</sup> The  
18 new tattoo battery displays limiting cycling capabilities and relatively higher internal resistance,  
19 reflected by the electrochemical impedance analysis of the battery (See supporting information,  
20 Figure S4). The capacity losses could arise during the fabrication process, use of gel electrolytes  
21 and due to the formation of resistive  $\text{Ag}_2\text{O}$  species at the positive electrode. The morphology  
22 changes of the anode and cathode after complete discharge also explains the capacity loss during  
23 cycling. Hydrogen evolution occurring at the negative electrode could be another reason for the  
24 capacity loss.

25

## 26 Conclusions

27 We have demonstrated the fabrication and operation of a non-toxic printable Ag-Zn  
28 tattoo battery that can be easily worn onto the skin to power wearable electronics. The work  
29 provides, for the first time, insights in the fabrication on printed wearable batteries using cost-  
30 effective screen printing and temporary tattoo technologies. The battery can be transferred on to  
31 body without the need of a special casing for the battery. The inexpensive tattoo paper aids the  
32 translation of conventional battery to a wearable design. The lateral disposition of the anode and  
33 cathode allows us to build the battery in arrays and to tune the power requirements at our will.  
34 The epidermal battery is rechargeable and its flexibility is demonstrated by repeated stretching  
35 and bending experiments. The performance of the tattoo battery (resiliency towards stretching  
36 stress, charge-discharging efficiency, etc) may be enhanced by further improving the design  
37 parameters including electrode architecture and types of electrolytes. This represents an  
38 important step towards building rechargeable batteries on temporary transfer tattoos for facile  
39 transfer to the skin ushering us towards “*tattootronics*” for flexible electronics.

1  
2  
3  
4  
5  
6  
7  
8  
9  
10  
11  
12  
13  
14  
15  
16  
17  
18  
19  
20  
21  
22  
23  
24  
25  
26  
27  
28  
29  
30  
31  
32  
33  
34  
35  
36  
37  
38

## Acknowledgement

This project was supported by National Science Foundation (Awards CBET-1066531). SB acknowledges USIEF for Fulbright-Nehru senior research fellowship and the Director Central Electrochemical Research Institute, Karaikudi, India, for sanctioning leave to avail the fellowship. Y.S. Meng acknowledges the Qualcomm gift fund. We thank S. Sattayasamitsathit and X. Wang for recording SEM images and preparation of reagents respectively.

## References

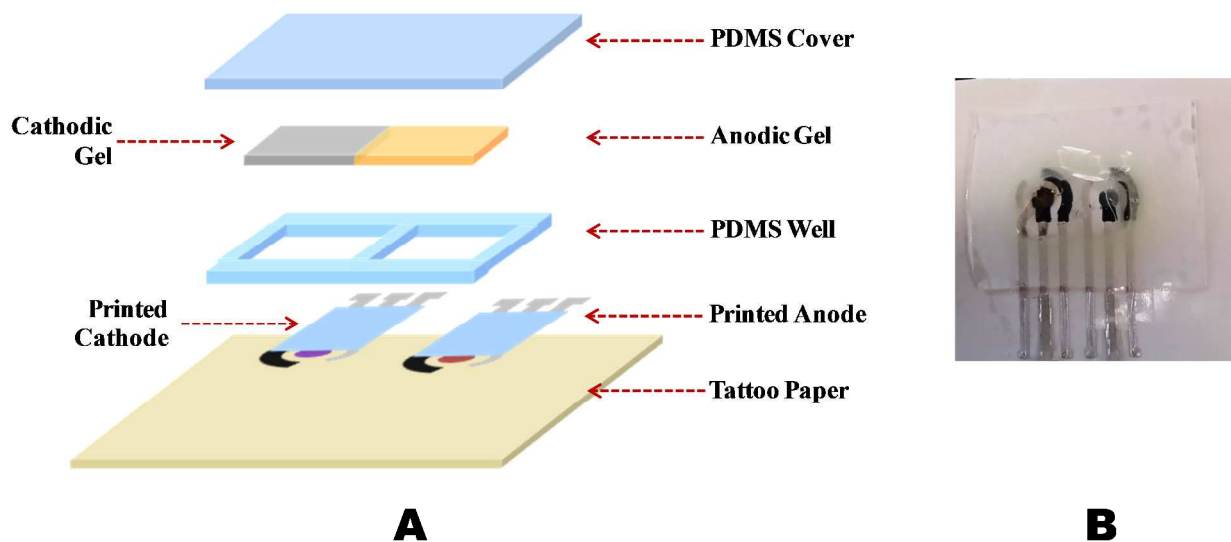
- [1] D. H. Kim, R. Ghaffari, N. Lu and J. A. Rogers, *Annu. Rev. Biomed. Eng.*, 2012, **14**, 113-128.
- [2] W. Jia, A. J. Bandodkar, G. Valdés-Ramírez, J. R. Windmiller, Z. Yang, J. Ramírez, G. Chan and J. Wang, *Anal. Chem.*, 2013, **85**, 6553–6560.
- [3] A. J. Bandodkar, V. W. S. Hung, W. Jia, G. Valdes-Ramírez, J. R. Windmiller, A. G. Martinez, J. Ramírez, G. Chan, K. Kerman and J. Wang, *Analyst*, 2013, **138**, 123–128.
- [4] A. J. Bandodkar, D. Molinnus, O. Mirza, T. Guinovart, J. R. Windmiller, G. Valdés-Ramírez, F. J. Andrade, M. J. Schöning and J. Wang, *Biosens. Bioelectron.*, 2014, **54**, 603–609.
- [5] A. M. Gaikwad, G. L. Whiting, D. A. Steingart and A. C. Arias, *Adv. Mater.*, 2011, **23**, 3251–2355.
- [6] C. Yan and P. S. Lee, *Small*, DOI: 10.1002/sml.201302806.
- [7] Y. Qin, X. D. Wang and Z. L. Wang, *Nature*, 2008, **451**, 809 – 813.
- [8] L. H. Zhang, E. Z. Shi, C. Y. Ji, Z. Li, P. X. Li, Y. Y. Shang, Y. B. Li, J. Q. Wei, K. L. Wang, H. W. Zhu, D. H. Wu and A. Y. Cao, *Nanoscale*, 2012, **4**, 4954 – 4959.
- [9] S. Zhang, C. Ji, Z. Bian, R. Liu, X. Xia, D. Yun, L. Zhang, C. Huang, and A. Cao, *Nano Lett.* 2011, **11**, 3383–3387
- [10] J. Bae, M. K. Song, Y. J. Park, J. M. Kim, M. L. Liu and Z. L. Wang, *Angew. Chem. Int. Ed.*, 2011, **50**, 1683 – 1687.
- [11] S. J. Kim, J. H. We and B. J. Cho, *Energy Environ. Sci.*, DOI: 10.1039/c4ee00242c

- 1  
2 [12] W. Jia, G. Valdés-Ramírez, A. J. Bando, J. R. Windmiller and J. Wang, *Angew.*  
3 *Chem. Int. Ed.*, 2013, **52**, 7233–7236.  
4
- 5 [13] P. P. Mercier, A. C. Lysaght, S. Bandyopadhyay, A. P. Chandrakasan and K. M.  
6 Stankovic, *Nat. Biotechnol.*, 2012, **30**, 1240–1243.  
7
- 8 [14] D. H. Kim, N. Lu, R. Ma, Y. S. Kim, R. H. Kim, S. Wang, J. Wu, S. M. Won, H. Tao, A.  
9 Islam, K. J. Yu, T. Kim, R. Chowdhury, M. Ying, L. Xu, M. Li, H. J. Chung, H. Keum, M.  
10 McCormick, P. Liu, Y. W. Zhang, F. G. Omenetto, Y. Huang, T. Coleman and J. A. Rogers,  
11 *Science*, 2011, **333**, 838–843.  
12
- 13 [15] S. Xu, Y. Zhang, J. Cho, J. Lee, X. Huang, L. Jia, J. A. Fan, Y. Su, J. Su, H. Zhang, H.  
14 Cheng, B. Lu, C. Yu, C. Chuang, T. Kim, T. Song, K. Shigeta, S. Kang, C. Dagdeviren,  
15 I. Petrov, P. V. Braun, Y. Huang, U. Paik and J. A. Rogers, *Nature Commun.*, 2013, **4**, 1–8.  
16
- 17 [16] Y. H. Lee, J. S. Kim, J. Noh, I. Lee, H. Jun Kim, S. Choi, J. Seo, S. Jeon, T. S. Kim, J. Y.  
18 Lee and J. W. Choi, *Nano Lett.* 2013, **13**, 5753–5761.  
19
- 20 [17] Z. Song, T. Ma, R. Tang, Q. Cheng, X. Wang, D. Krishnaraju, R. Panat, C. K. Chan, H.  
21 Yu and H. Jiang, *Nature Commun.*, DOI: 10.1038/ncomms4140.  
22
- 23 [18] L. Hu, H. Wu, F. L. Mantia, Y. Yang and Y. Cui, *ACS Nano*, 2010, **4**, 5843–5848.  
24
- 25 [19] V. L. Pushparaj, M. M. Shaijumon, A. Kumar, S. Murugesan, L. Ci, R. Vajtai, R. J.  
26 Linhardt, O. Nalamasu and P. M. Ajayan, *PNAS*, 2007, **104**, 13574–13577.  
27
- 28 [20] Y. H. Kwon, S-W. Woo, H. R. Jung, H. K. Yu, K. Kim, B. H. Oh, S. Ahn, S. Y. Lee, S.  
29 W. Song, J. Cho, H. C. Shin and J. Y. Kim, *Adv. Mater.*, 2012, **24**, 5192–5197.  
30
- 31 [21] P. Hiralal, S. Imaizumi, H. E. Unalan, H. Matsumoto, M. Minagawa, M. Rouvala, A.  
32 Tanioka and G. A. J. Amaratunga, *ACS Nano*, 2010, **4**, 2730–2734.  
33
- 34 [22] M. Kaltenbrunner, G. Kettlgruber, C. Siket, R. Schwödiauer and S. Bauer, *Adv. Mater.*,  
35 2010, **22**, 2065–2067.  
36
- 37 [23] A. M. Gaikwad, D. A. Steingart, T. N. Ng, D. E. Schwartz and G. L. Whiting, *Appl.*  
38 *Phys. Lett.*, 2013, **102**, 233302–233306.  
39

- 1 [24] A. M. Gaikwad, H. N. Chu, R. Qeraj, A. M. Zamarayeva and D. A. Steingart, *Ener.*  
2 *Technol.*, 2013, **1**, 177–185.
- 3
- 4 [25] G. Kettlgruber, M. Kaltenbrunner, C. M. Siket, R. Moser, I. M. Graz, R. Schwödauer  
5 and S. Bauer, *J. Mater. Chem. A*, 2013, **1**, 5505–5508.
- 6
- 7 [26] C. Yan, X. Wang, M. Cui, J. Wang, W. Kang, C. Y. Foo and P. S. Lee, *Adv. Energy*  
8 *Mater.*, DOI: 10.1002/aenm.201470020.
- 9
- 10 [27] M. Hilder, B. Winther-Jensen and N. B. Clark, *J. Power Sources*, 2009, **194**, 1135–1141.
- 11
- 12 [28] I. Ferreira, B. Brás, N. Correia, P. Barquinha, E. Fortunato and R. Martins, *J. Display*  
13 *Technol.*, 2010, **6**, 332–335.
- 14
- 15 [29] I. Ferreira, B. Brás, J. I. Martins, N. Correia, P. Barquinha, E. Fortunato and R. Martins,  
16 *Electrochim. Acta*, 2011, **56**, 1099–1105.
- 17
- 18 [30] K. B. Lee, *J. Micromech. Microeng.*, 2005, **15**, S210–S214.
- 19
- 20 [31] K. B. Lee, *J. Micromech. Microeng.*, 2006, **16**, 2312–2317.
- 21
- 22 [32] N. K. Thom, K. Yeung, M. B. Phillion and S. T. Phillips, *Lab Chip*, 2012, **12**, 1768–1770.
- 23
- 24 [33] N. K. Thom, G. G. Lewis, M. J. Di Tucci and S. T. Phillips, *RSC Adv.*, 2013, **3**, 6888–  
25 6895.
- 26
- 27 [34] X. Zhang, J. Li, C. Chen, B. Lou, L. Zhang and E. Wang, *Chem. Commun.*, 2013, **49**,  
28 3866–3868.
- 29
- 30 [35] X. Zhang, Z. Lin, B. Chen, S. Sharma, C. Wong and Y. Deng *J. Mater. Chem. A*, 2013, **1**,  
31 5835–5839.
- 32
- 33 [36] H. Liu and R. M. Crooks, *Anal. Chem.*, 2012, **84**, 2528–2532.
- 34
- 35 [37] P. Suresh, D. H. Nagaraju, A. K. Shukla, N. Munichandraiah, *Electrochim. Acta*, 2005,  
36 **50** 3262–3272.
- 37
- 38 [38] J. R. Windmiller, A. J. Bandodkar, G. Valdés-Ramírez, S. Parkhomovsky, A. G. Martinez  
39 and J. Wang. *Chem. Comm.*, 2012, **48**, 6794–6796.
- 40

- 1 [39] K. T. Braam, S. K. Volkman, V. Subramanian, *J. Power Sources*, 2012, **199**, 367–372.  
2  
3 [40] J. K. Kim, A. Armutlulu, M. Kim, S. Paik, S. A. B. Allen and M. G. Allen, *Power*  
4 *MEMS*, 2012, 371–374.  
5  
6 [41] D. Coates, E. Ferreira and A. Charkey, *J. Power Sources*, 1997, **65**, 109–115.  
7  
8  
9





1  
2  
3  
4  
5  
6  
7  
8  
9  
10  
11  
12  
13  
14  
15  
16  
17  
18  
19  
20  
21  
22  
23  
24  
25  
26

Figure 1 (A) Schematic diagram illustrating the different steps involved in the fabrication of the Ag-Zn cell. (B) The prototype of the Ag-Zn cell on temporary transfer tattoo support.

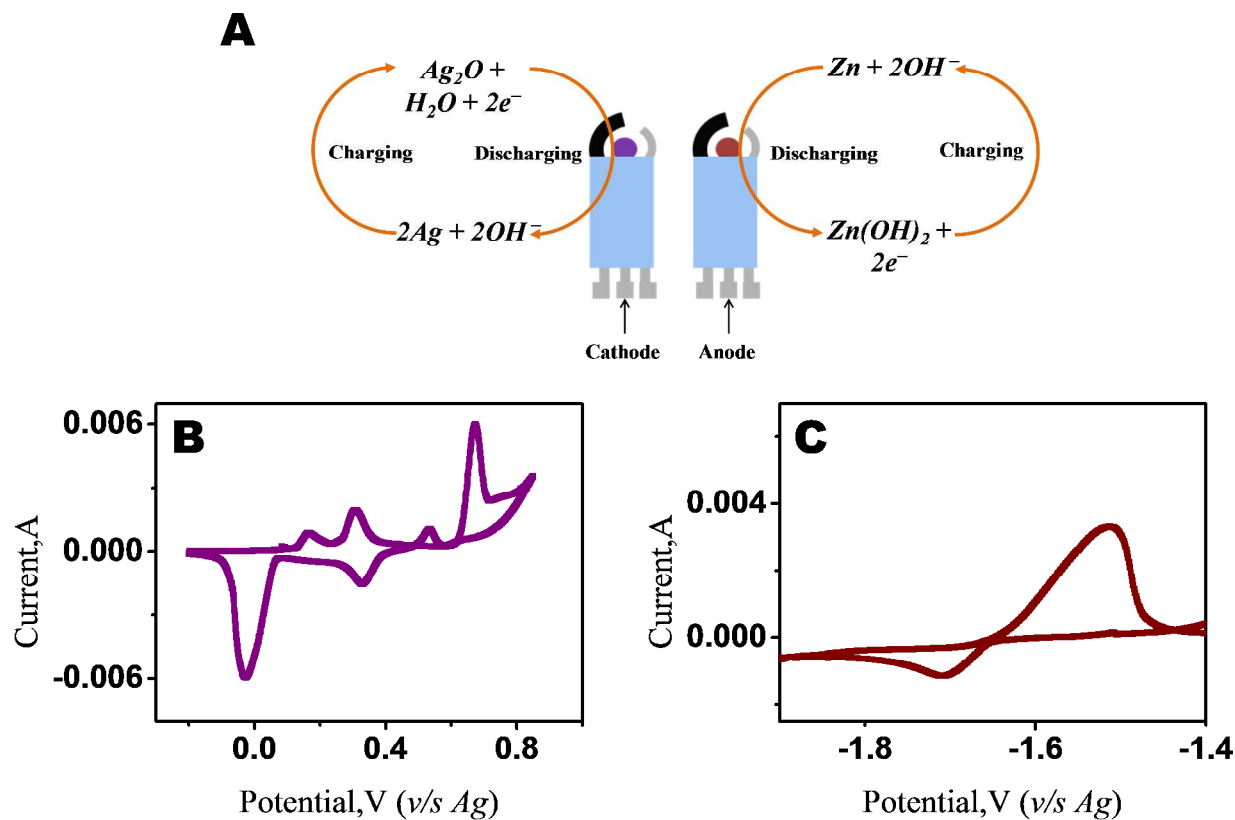
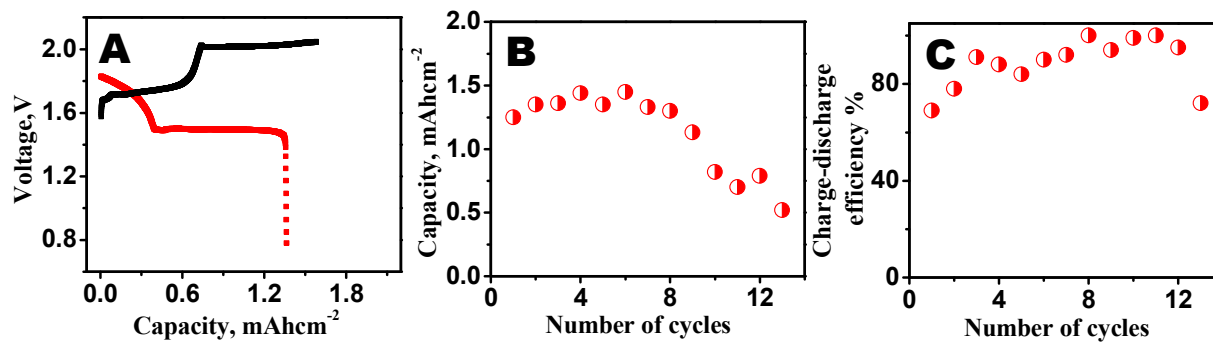
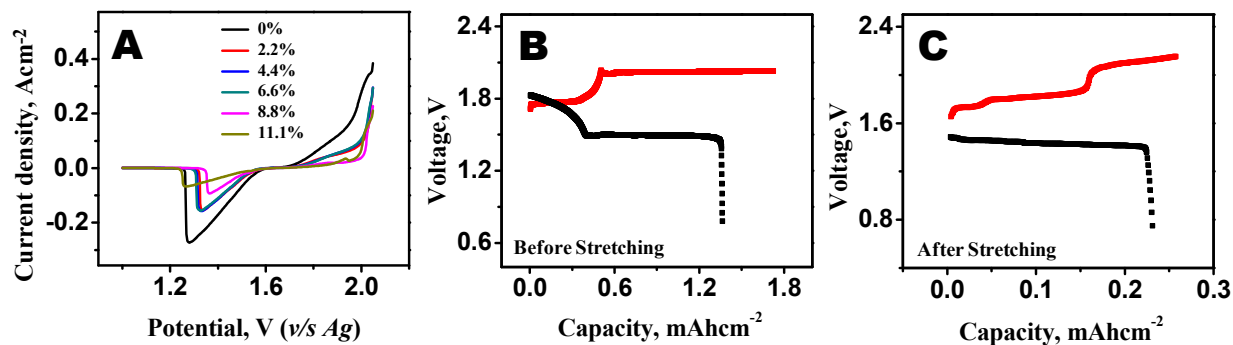


Figure 2 (A) Typical redox reactions at the negative and positive electrodes. (B) Cyclic voltammetric response of the negative Zn electrode. (C) Cyclic voltammetric response of the positive Ag electrode in 6 M KOH +1M LiOH at 5 mV/s.

1  
2  
3  
4  
5  
6  
7  
8  
9  
10  
11  
12  
13  
14  
15

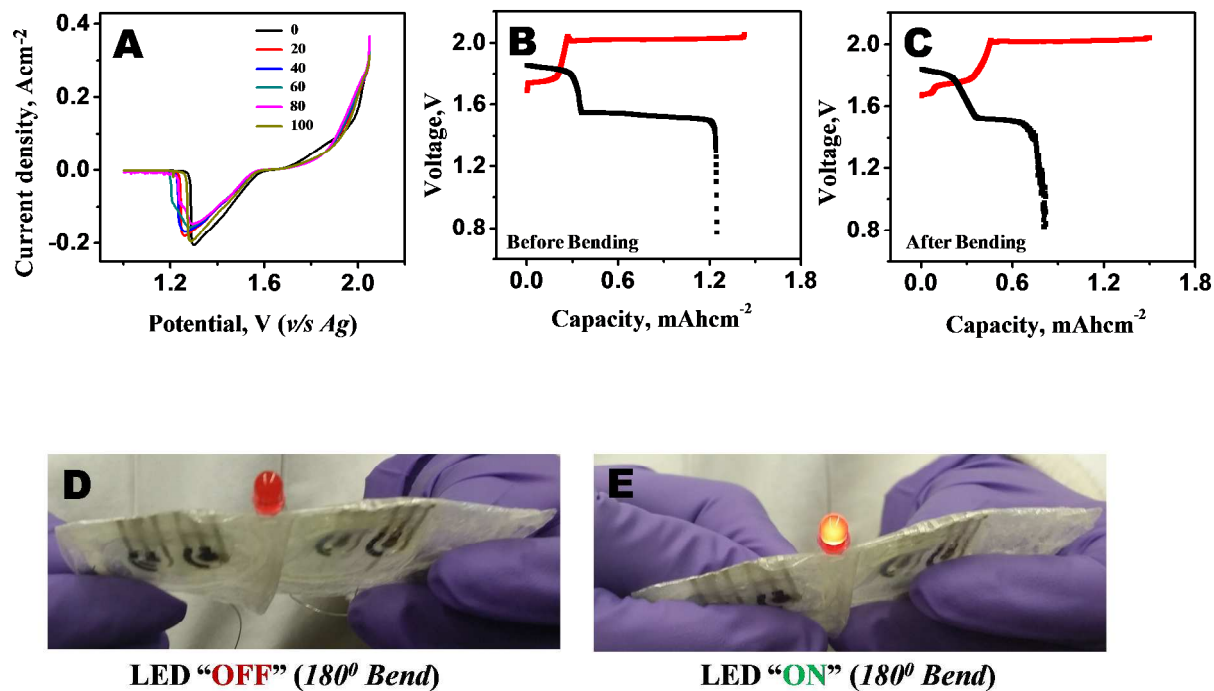


1  
2 Figure 3 (A) Typical charge–discharge characteristic of an Ag-Zn tattoo cell. (B) Discharge  
3 capacity vs number of cycles. (C) Charge-Discharge efficiency vs number of cycles.  
4  
5  
6  
7  
8  
9  
10  
11  
12  
13  
14  
15  
16  
17  
18  
19  
20  
21



1  
2 Figure 4 (A) Linear sweep discharge curves at 2mV/s for different percentages of stretching. (B)  
3 Galvanostatic charge-discharge before discharge experiments. (C) Galvanostatic charge-  
4 discharge after stretching experiments. Red plot corresponds to the charging curve while black  
5 plot corresponds to the discharge curve in figures B and C.

6  
7  
8  
9  
10  
11  
12  
13  
14  
15  
16  
17  
18  
19  
20  
21  
22

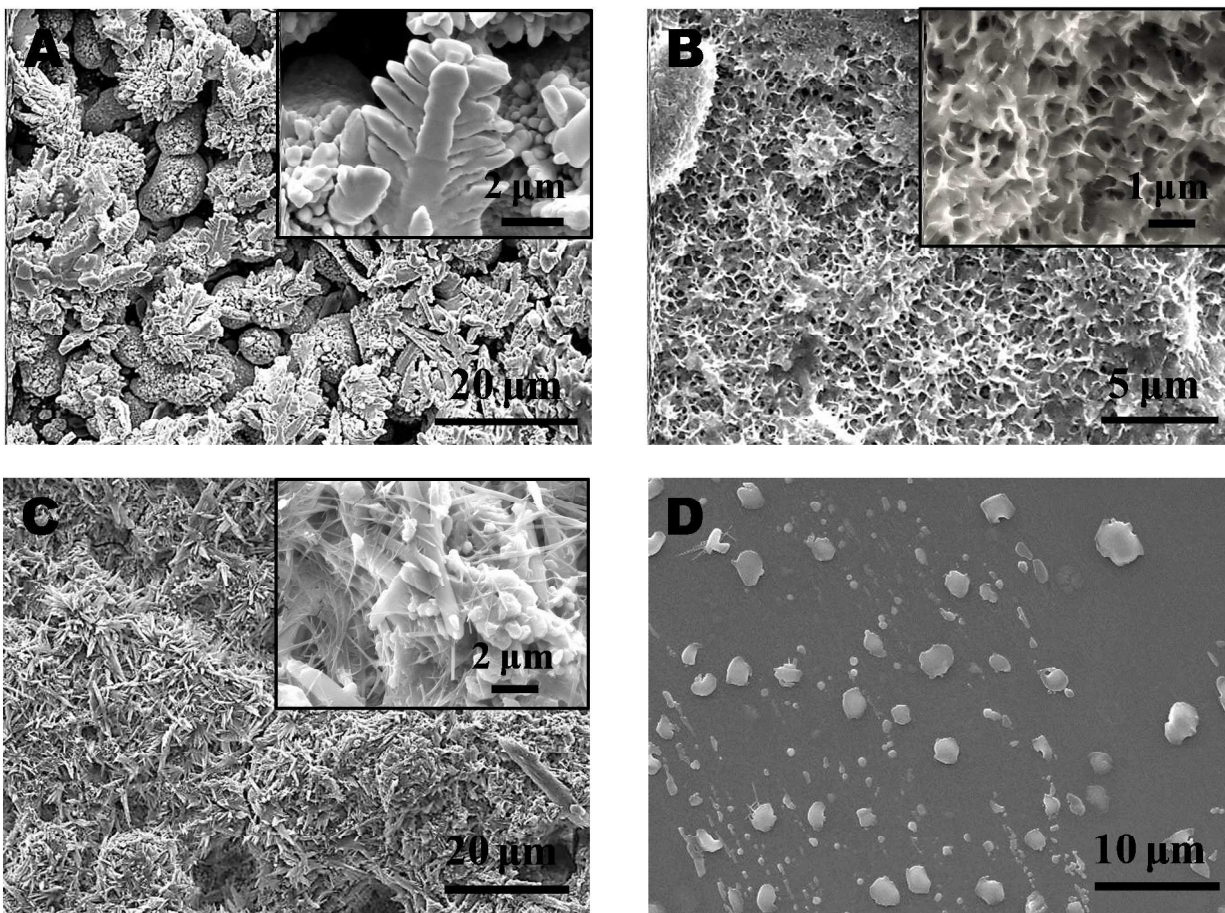


LED "OFF" (180° Bend)

LED "ON" (180° Bend)

1  
2  
3 Figure 5 (A) Linear sweep discharge curves at 2 mV/s recorded over 5 bend cycles. (B)  
4 Galvanostatic discharge before bending. (C) Galvanostatic discharge after bending. (D-G)  
5 Demonstration of the performance of the tattoo battery under deformed conditions. Red plot  
6 corresponds to the charging curve while the black plot corresponds to the discharge curve in  
7 figures B and C.

8  
9  
10  
11  
12  
13  
14  
15



1  
2 Figure 6: SEM images of (A) electrodeposited Ag electrode on carbon current collector (*inset*:  
3 Zoomed in image of the Ag electrode). (B) Ag electrode after complete discharge (*inset*:  
4 Zoomed in image of the Ag electrode). (C) Electrodeposited Zn electrode on carbon current  
5 electrode (*inset*: Zoomed in image of the Zn electrode). (D) Zn electrode after discharge.  
6  
7  
8  
9  
10  
11  
12  
13  
14



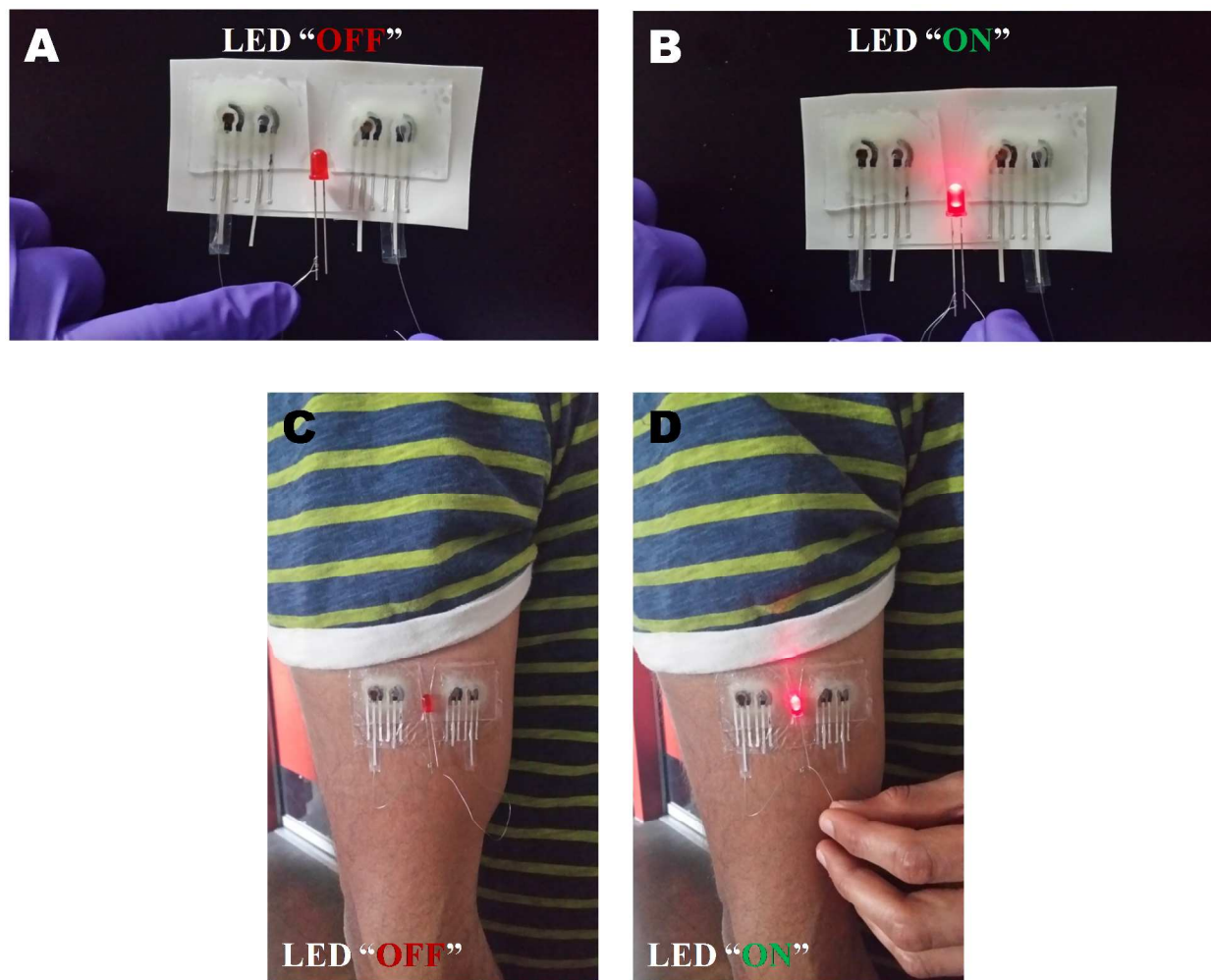


Figure 7 Demonstration of practical utility of the tattoo battery for lighting a red LED (A, B) before transfer onto skin (C, D) after transfer onto skin.

1  
2  
3  
4  
5  
6  
7  
8  
9  
10  
11  
12  
13  
14  
15